

# Nitric Oxide-Releasing Xerogel Microarrays Prepared with Surface-Tailored Poly(dimethylsiloxane) Templates

Mary E. Robbins, Bong Kyun Oh, Erin D. Hopper, and Mark H. Schoenfish\*

Department of Chemistry, University of North Carolina at Chapel Hill,  
Chapel Hill, North Carolina 27599-3290

Received February 18, 2005. Revised Manuscript Received March 31, 2005

Surface graft polymerization with poly(ethylene glycol) acrylate is reported as an effective method for modifying the surface of poly(dimethylsiloxane) array templates thus enabling the preparation of nitric oxide (NO)-releasing xerogel micropatterns. The surface wettability of PEGA-grafted templates was sufficient to overcome the flow resistance of ethyltrimethoxysilane (ETMOS) sol solutions and allow the formation of xerogel microarrays via capillary action of sol through the template channels. Due to the combined versatility of both sol–gel chemistry and micropatterning, substrates were modified with a range of aminosilane-doped xerogel microarrays with variable NO release properties. Several parameters were studied including (1) NO surface flux as a function of type and concentration of aminosilane NO-donor precursor; (2) micropattern dimensions for maximizing surface flux and duration of NO release; and (3) the effect of microstructure separation on localized NO surface concentration as determined with a NO-selective ultramicroelectrode sensor. Xerogel microarrays were characterized by initial NO surface fluxes ranging from  $3.9 \pm 0.5$  to  $73.6 \pm 5.7$   $\text{pmol}\cdot\text{cm}^{-2}\cdot\text{s}^{-1}$ . Although the NO surface flux subsided with time as the finite reservoir within the xerogel became depleted, the duration of measurable NO release was double that of previously reported MTMOS arrays. Thus, NO-releasing aminosilane-modified ETMOS arrays may represent a promising strategy for further improving the in vivo biocompatibility of implantable sensors.

## Introduction

Despite significant progress in recent years toward the development of more biocompatible polymer coatings for medical implant devices, the in vivo utility of such materials for sensor applications remains limited. Biofouling due to surface-induced thrombosis (blood clot formation) and implant-associated infection continues to hinder the long-term use of in vivo sensors.<sup>1,2</sup> Polymers designed to slowly release nitric oxide (NO) have emerged as a class of materials well-suited for biomedical applications due to the role of endogenously produced NO in numerous physiological processes including the regulation of platelet adhesion and activation,<sup>3</sup> angiogenesis (formation of new blood capillaries),<sup>4</sup> phagocytosis (digestion of bacteria),<sup>5</sup> and wound healing.<sup>6</sup> Since the half-life of NO is extremely short in biological milieu,<sup>7</sup> the effects of NO are localized at the implant surface and the potential health risks associated with systemic anticoagulant and antibiotic therapies are avoided.

Nitric oxide-releasing polymers have been incorporated into a variety of sensing devices including ion-selective electrodes for  $\text{H}^+$  and  $\text{K}^+$ ,<sup>8</sup> optical<sup>9</sup> and amperometric<sup>10–13</sup> oxygen sensors, and enzymatic glucose biosensors.<sup>14,15</sup> Promising in vitro and in vivo performance and biocompatibility have been observed for short-term applications (several hours). However, the improved biocompatibility is not sustained upon depletion of the finite NO reservoir within the polymer.<sup>12,15</sup> Enhanced NO release may be achieved by varying the NO donor and/or increasing the NO donor loading rate and polymer film thickness.<sup>16</sup> To date, polymer/material stability dictates NO donor loading limitations. In addition, thicker films pose a more substantial barrier to mass transport for sensing applications that rely on analyte diffusion to the sensor surface.<sup>1</sup>

\* To whom correspondence should be addressed. E-mail: schoenfi@email.unc.edu.

- (1) Frost, M. C.; Meyerhoff, M. E. *Curr. Opin. Chem. Biol.* **2002**, *6*, 633–641.
- (2) Keefer, L. K. *Annu. Rev. Pharmacol. Toxicol.* **2003**, *43*, 585–607.
- (3) Radomski, M. W.; Rees, D. D.; Dutra, A.; Moncada, S. *Br. J. Pharmacol.* **1992**, *107*, 745–749.
- (4) Rudic, R. D.; Shelsey, E. G.; Maeda, N.; Smithies, O.; Segal, S. S.; Sessa, W. C. *J. Clin. Invest.* **1998**, *101*, 731–736.
- (5) Albina, J. E.; Reichner, J. S. *Cancer Metastasis Rev.* **1998**, *17*, 19–53.
- (6) Efron, D.; Most, D.; Barbul, A. *Curr. Opin. Clin. Nutr. Metab. Care* **2000**, *3*, 197–204.
- (7) Kelm, M.; Yoshida, K. In *Methods in Nitric Oxide Research*; Feelisch, M., Stamler, J. S., Eds.; John Wiley: New York, 1996; pp 47–58.

- (8) Espadas-Torre, C.; Oklejas, V.; Mowery, K. A.; Meyerhoff, M. E. *J. Am. Chem. Soc.* **1997**, *119*, 2321–2322.
- (9) Schoenfish, M. H.; Zhang, H. Z.; Frost, M. C.; Meyerhoff, M. E. *Anal. Chem.* **2002**, *74*, 5937–5941.
- (10) Mowery, K. A.; Schoenfish, M. H.; Narayan, B.; Wahr, J. A.; Meyerhoff, M. E. *Electroanalysis* **1999**, *11*, 681–686.
- (11) Schoenfish, M. H.; Mowery, K. A.; Rader, M.; Baliga, N.; Wahr, J.; Meyerhoff, M. E. *Anal. Chem.* **2000**, *72*, 1119–1126.
- (12) Frost, M. C.; Rudich, S. M.; Zhang, H. Z.; Maraschio, M. A.; Meyerhoff, M. E. *Anal. Chem.* **2002**, *74*, 5942–5947.
- (13) Marxer, S. M.; Robbins, M. E.; Schoenfish, M. H. *Analyst* **2005**, *130*, 206–212.
- (14) Shin, J. H.; Marxer, S. M.; Schoenfish, M. H. *Anal. Chem.* **2004**, *76*, 4543–4549.
- (15) Oh, B. K.; Robbins, M. E.; Nablo, B. J.; Schoenfish, M. H. *Biosens. Bioelectron.* **2005**, in press.
- (16) Zhang, H.; Annich, G. M.; Miskulin, J.; Osterholzer, K.; Merz, S. I.; Bartlett, R. H.; Meyerhoff, M. E. *Biomaterials* **2002**, *23*, 1485–1494.

We recently reported the use of micropatterning methods as a means for selectively modifying substrates with precisely positioned NO-releasing xerogel microstructures, whereby regions of the underlying surface remain unmodified (i.e., between the xerogel features).<sup>17–19</sup> Methyltrimethoxysilane (MTMOS) xerogels doped with varying concentrations of AEMP3 were employed in these studies since patterning this particular sol was straightforward.<sup>17–19</sup> In vitro platelet adhesion experiments confirmed that at a NO surface flux of  $2.2 \text{ pmol}\cdot\text{cm}^{-2}\cdot\text{s}^{-1}$ , arrays of xerogel lines separated by up to  $50 \mu\text{m}$  were equally as thromboresistant as uniform xerogel coatings (i.e., NO-releasing films).<sup>17,18</sup> When the microstructure separation was reduced to  $10 \mu\text{m}$ , a NO surface flux of only  $0.42 \text{ pmol}\cdot\text{cm}^{-2}\cdot\text{s}^{-1}$  effectively prevented platelet adhesion.<sup>18</sup> Similar results were reported for in vitro bacterial adhesion by Dobmeier et al.<sup>19</sup> A 50% reduction in *Pseudomonas aeruginosa* adhesion to NO-releasing ( $1.0 \text{ pmol}\cdot\text{cm}^{-2}\cdot\text{s}^{-1}$ ) arrays was observed with microstructure separations up to  $200 \mu\text{m}$ .<sup>19</sup> These findings suggest that substrates modified with NO-releasing xerogel arrays may be useful for improving the biocompatibility of an interface while preserving the properties (e.g., functionality) of the underlying surface. Indeed, electrodes modified with arrays of xerogel lines ( $5 \mu\text{m}$  wide) separated by  $5 \mu\text{m}$  of exposed platinum exhibited a 4-fold increase in oxygen response relative to xerogel-coated electrodes.<sup>18</sup> This increase was attributed to enhanced analyte mass transport to the electrode surface in regions between xerogel lines. As expected, the oxygen response was further enhanced as the microstructure separation was increased from  $5$  to  $20 \mu\text{m}$ , albeit at the expense of surface thromboresistivity.<sup>18</sup>

Similarly, a miniaturized enzymatic glucose biosensor modified with a NO-releasing xerogel microarray was characterized by significantly higher sensitivity ( $0$ – $20 \text{ mM}$  glucose) than a comparable sensor modified with a xerogel film.<sup>15</sup> While the response of the xerogel-coated sensor decreased by  $>99\%$  relative to the control sensor, the sensitivity of the micropatterned sensor ( $20 \mu\text{m}$  microstructure separations) was reduced by only  $36\%$ .<sup>15</sup> The patterned biosensor exhibited a sensitive ( $0.194 \pm 0.033 \text{ nA/mM}$  glucose) and linear response that was stable for  $7 \text{ d}$ , and in vitro studies confirmed that the NO-releasing micropatterned surfaces were significantly more resistant to both platelet and bacterial adhesion than controls.<sup>15</sup> Unfortunately, NO release longevity from such patterns was limited due to the sol composition, ultimately leading to increased platelet and bacterial adhesion at long immersion times. Thus, the utility of xerogel micropatterns for enhancing the biocompatibility of implantable sensors relies on the synthesis of arrays with greater NO-release capability.

Herein, we report on the synthesis and characterization of aminosilane-modified ethyltrimethoxysilane (ETMOS) xerogel materials capable of releasing therapeutic levels of NO for several days. To compensate for the increased sol

viscosity (relative to MTMOS) and allow for effective patterning, the surface wettability of the elastomeric array template was increased using ultraviolet polymer grafting.<sup>20</sup> The optimum grafting conditions for effectively patterning aminosilane-doped ETMOS xerogels are discussed. Furthermore, we present a systematic study of the effects of the xerogel composition and microarray dimensions on the NO-release properties of aminosilane-modified ETMOS micropatterns.

## Experimental Section

**Materials.** (Aminoethylaminomethyl)phenethyltrimethoxysilane (AEMP3), *N*-(2-aminoethyl)-3-aminopropyltrimethoxysilane (AEAP3), *N*-(6-aminoethyl)aminopropyltrimethoxysilane (AHAP3), 3-aminopropyltrimethoxysilane (APTS), ethyltrimethoxysilane (ETMOS), and (heptadecafluoro-1,1,2,2-tetra-hydrodecyl)trichlorosilane were purchased from Gelest (Tullytown, PA). The aminosilane structures are shown in Figures 2A–C. Acrylic acid (AA), benzyl alcohol, dimethylacrylamide (DMA), ethanol (absolute, EtOH), sodium periodate, and Sylgard 184 (poly(dimethylsiloxane), PDMS) were purchased from Fisher Scientific (Philadelphia, PA). Methocel, poly(ethylene glycol) acrylate (PEGA), and silver (Ag) wire ( $76 \mu\text{m}$  outer diameter, o.d.) were supplied by Aldrich (St. Louis, MO). Platinum (Pt) wire ( $25 \mu\text{m}$  o.d.) was purchased from Alfa Aesar (Ward Hill, MA). Borosilicate glass capillaries ( $1 \text{ mm}$  o.d.) and RTV-3140 silicone rubber were obtained from World Precision Instruments Inc. (Sarasota, FL) and Dow Corning (Midland, MA), respectively. Nitric oxide (NO), argon (Ar), and nitrogen ( $\text{N}_2$ ) were purchased from National Welders Supply (Raleigh, NC). Silicon master templates prepared using conventional photolithography methods were obtained from MCNC (Research Triangle Park, NC). Distilled water was purified to  $18.2 \text{ M}\Omega\cdot\text{cm}^{-1}$  with a Millipore Milli-Q Gradient A-10 system (Bedford, MA). All other solvents and chemicals were analytical-reagent grade and used as received.

**Synthesis of Nitric Oxide-Releasing Xerogels.** Several aminosilane-modified ETMOS xerogels were synthesized by varying the silane composition from  $10$  to  $60\%$  aminosilane (v/v; balance ETMOS). The sol solution was prepared by combining  $200 \mu\text{L}$  of ethanol (EtOH),  $10 \mu\text{L}$  of water,  $10 \mu\text{L}$  of hydrochloric acid (HCl,  $0.5 \text{ M}$ ), and ETMOS ( $80$ – $180 \mu\text{L}$ ). This solution was mixed for  $1 \text{ h}$  before adding  $20$ – $120 \mu\text{L}$  of AEMP3, AEAP3, or AHAP3 (for a total silane volume of  $200 \mu\text{L}$ ) and mixing for an additional hour. Glass substrates ( $25 \text{ mm} \times 8 \text{ mm}$ ) were sonicated in EtOH for  $20 \text{ min}$ , rinsed with EtOH, dried under a stream of  $\text{N}_2$ , and ozone-cleaned for  $20 \text{ min}$  in a BioForce TipCleaner (Ames, IA). Xerogel films (thickness  $\sim 60 \mu\text{m}$ ) were prepared by casting  $30 \mu\text{L}$  of the sol solution onto the surface of the clean glass substrate. The xerogel-modified surfaces were cured for  $48 \text{ h}$  under ambient conditions. Diamine groups in the cured xerogel were then converted to diazeniumdiolate NO donors in an in-house reactor.<sup>21</sup> The reaction chamber was flushed thoroughly with Ar to remove air and moisture and pressurized with  $5 \text{ atm NO}$ . After  $3 \text{ d}$ , the reaction chamber was flushed thoroughly with Ar. The diazeniumdiolate-modified xerogels were then removed and stored in a sealed container at  $-20 \text{ }^\circ\text{C}$  until use.

**Micropatterning Xerogels.** Silicon (Si) wafers etched with arrays of rectangular channels were cleaned of residual organic contaminants by immersion in Piranha solution consisting of a  $3:7$

(17) Robbins, M. E.; Schoenfish, M. H. *J. Am. Chem. Soc.* **2003**, *125*, 6068–6069.

(18) Robbins, M. E.; Hopper, E. D.; Schoenfish, M. H. *Langmuir* **2004**, *20*, 10296–10302.

(19) Dobmeier, K. P.; Schoenfish, M. H. *Biomacromolecules* **2004**, *5*, 2493–2495.

(20) Hu, S.; Ren, X.; Bachman, M.; Sims, C. E.; Li, G. P.; Allbritton, N. L. *Anal. Chem.* **2002**, *74*, 4117–4123.

(21) Hrabie, J. A.; Klose, J. R.; Wink, D. A.; Keefer, L. K. *J. Org. Chem.* **1993**, *58*, 1472–1476.

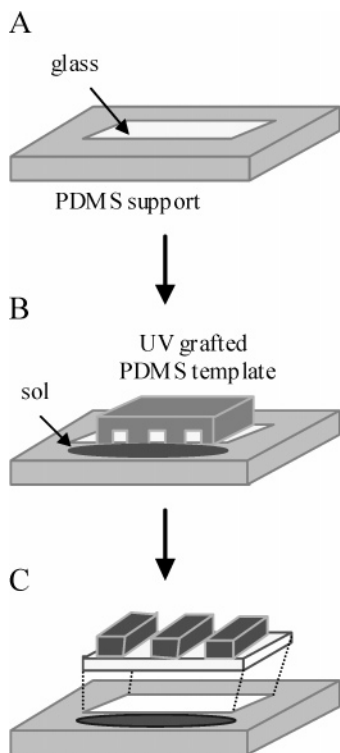


**Figure 1.** Schematic representation of xerogel microarray preparation in which (A) glass is embedded in an elastomeric PDMS support, followed by (B) placement of a UV grafted template in conformal contact with the glass surface, yielding an array of channels, which spontaneously fill with sol solution via capillary action. After curing, (C) the micropatterned substrate is removed from the support.

mixture (v/v) of H<sub>2</sub>O<sub>2</sub> (30%) and sulfuric acid (H<sub>2</sub>SO<sub>4</sub>, ~18 M). Care should be taken when using Piranha solution since it is a very strong oxidant and can spontaneously detonate upon contact with organic material. The Si was then rinsed thoroughly with water and EtOH, and dried under a stream of N<sub>2</sub>. To prevent bonding between PDMS and the Si surface, the wafers were incubated in (heptadecafluoro-1,1,2,2-tetra-hydrodecyl)-trichlorosilane vapor for 1 h in a N<sub>2</sub> environment.<sup>22</sup> The PDMS precursor and cross-linking solutions were combined in a 10:1 ratio, mixed thoroughly, and poured over the Si wafer or a clean flat dish (for materials characterization) to yield a layer with thickness ~5 mm. The mixture was degassed under vacuum for 30 min, and cured at 70 °C overnight. The elastomeric templates were then removed from the Si wafer or flat dish, rinsed with EtOH, and dried in a stream of N<sub>2</sub>. To increase surface hydrophilicity, the PDMS templates were modified according to the method described by Hu et al.<sup>20</sup> Briefly, micropatterned and smooth templates were placed in a quartz reaction tube and immersed in an aqueous solution of sodium periodate (0.5 mM), benzyl alcohol (1 wt %), and either AA, DMA, or PEGA (10 wt %). The reaction tube, containing the samples, was then placed in a home-built ultraviolet (UV) reactor equipped with a 200-W mercury vapor lamp housed within a quartz immersion well (Ace Glass, Vineland, NJ). The reaction tube was positioned at a distance of 7 cm from the UV lamp for 1–4 h. The templates were then removed, immersed in water at 80 °C overnight to rinse adsorbed monomeric or polymeric species, and dried in a stream of N<sub>2</sub>. Xerogel micropatterns were prepared by placing a micromolded template in conformal contact with a cleaned glass substrate previously embedded in a PDMS support as shown schematically in Figure 1.<sup>18</sup> Sol deposited on the PDMS base was

then drawn into the microchannels by capillary action.<sup>17,18</sup> After curing for 48 h under ambient conditions, the template was removed to reveal the xerogel microarray. Excess xerogel was separated from the micropattern by removing the glass substrate from the elastomeric support. The diamine precursors in the xerogel micropatterns were converted to diazeniumdiolate NO donors as described above.

**Material Characterization.** The rate and duration of NO release from modified xerogels were determined using a Sievers NOA 280i chemiluminescence nitric oxide analyzer (Boulder, CO). Xerogel films and microarrays were placed in a reaction cell containing 15 mL of Tyrode's buffer (137 mM sodium chloride, 5.6 mM D-(+)-glucose, 3.3 mM potassium phosphate monobasic, and 2.7 mM potassium chloride; pH 7.4) at 37 °C. Nitric oxide released from the xerogel was transported to the analyzer by a stream of N<sub>2</sub> passed through the reaction cell. The level of NO (ppb) was measured in real-time and used to calculate the NO surface flux (pmol·cm<sup>-2</sup>·s<sup>-1</sup>).

The surface wettability of the xerogel films and the flat PDMS templates was evaluated before and after NO-donor formation and UV-grafting, respectively. Static water contact angles were obtained using a KSV Instruments Cam 200 optical contact angle meter (Helsinki, Finland).

Xerogel stability was evaluated by casting films onto glass slides that were previously cleaned in 10% nitric acid (v/v, water) for 20 min at 80 °C, followed by sequential immersion in 10% APTS (v/v, water, pH 6.5) for 1 h at 80 °C and 10% glutaraldehyde (v/v, water) for 1 h at room temperature.<sup>23</sup> The surfaces were rinsed thoroughly with water, dried in a stream of N<sub>2</sub>, and modified with a xerogel coating. Following curing and exposure to high pressures of NO (as described above), the substrates were immersed in Tyrode's buffer at 37 °C for 1–14 d. The concentration of Si in the soak solutions, a measure of xerogel fragmentation, was determined using an ARL-Fisons Spectrascan 7 direct current plasma optical emission spectrometer (DCP-OES; Beverly, MA). The instrument, which has a detection limit of 0.4 ppm, was calibrated with the following standard solutions; 0.0, 1.0, 2.0, 5.0, 10.0, 25.0, and 50.0 ppm Si in Tyrode's buffer. The extent of fragmentation was calculated as μmol Si per unit area of xerogel film (μmol·cm<sup>-2</sup>).

Micropattern surface topography was characterized using a PicoSPM (Molecular Imaging; Tempe, AZ) atomic force microscope (AFM) in contact mode. The spring constant of the Si<sub>3</sub>N<sub>4</sub> AFM probes was approximately 0.12 N/m. The root-mean-square (rms) roughness of the xerogel surfaces was calculated using Molecular Imaging Visual SPM software. The lateral dimensions and uniformity of xerogel microarrays were evaluated with phase contrast optical micrographs obtained using a Zeiss Axiovert 200 inverted microscope (Chester, VA).

**Nitric Oxide Surface Concentration Measurements.** A miniaturized planar amperometric NO sensor was prepared as described elsewhere.<sup>24</sup> Briefly, glass-sealed Pt and coiled Ag wires served as the working and reference electrodes, respectively. The reference electrode was immobilized in close proximity to the working electrode using silver paint. The diameter of the sensing tip was minimized by mechanically polishing the insulating glass sheath to achieve a conical shape with a final tip diameter of ca. 50 μm. The sensing tip was then coated with an internal hydrogel layer containing 1 wt % Methocel, 30 mM sodium chloride (NaCl), and 0.3 mM HCl, pH 3.5. An outer silicone rubber gas permeable membrane was then formed by dip-coating the sensor in a 1% (w/v) solution of RTV-3140 in tetrahydrofuran. After drying overnight, the NO sensor was immersed in phosphate buffered saline (PBS,

(22) James, C. D.; Davis, R. C.; Kam, L.; Craighead, H. G.; Isaacson, M. *Langmuir* **1998**, *14*, 741–744.

(23) Chowdhury, P. B.; Luckham, P. F. *Colloids Surf., A* **1998**, *143*, 53–57.

(24) Oh, B. K.; Robbins, M. E.; Schoenfisch, M. H. **2005**, in preparation.

**Table 1. Nitric Oxide Surface Flux ( $\text{pmol}\cdot\text{cm}^{-2}\cdot\text{s}^{-1}$ ) from AEMP3, AEAP3, and AHAP3 (Balance ETMOS) Xerogel Films as Measured by Chemiluminescence<sup>a</sup>**

% (v/v)	0 h	8 h	2 d	4 d	6 d	8 d
			AEMP3			
10	4.9 ± 1.2	0.9 ± 0.1	<0.1 <sup>b</sup>	<0.1	<0.1	<0.1
20	7.6 ± 0.8	1.3 ± 0.3	0.3 ± 0.1	<0.1	<0.1	<0.1
40	9.1 ± 0.2	4.1 ± 0.2	0.3 ± 0.1	0.2 ± 0.1	<0.1	<0.1
60	17.7 ± 1.5	10.1 ± 1.3	0.5 ± 0.3	0.2 ± 0.1	<0.1	<0.1
			AEAP3			
10	15.5 ± 1.6	5.2 ± 0.9	0.9 ± 0.5	<0.1	<0.1	<0.1
20	30.6 ± 2.2	11.9 ± 1.4	1.9 ± 0.2	0.2 ± 0.1	<0.1	<0.1
40	75.5 ± 7.6	44.1 ± 3.4	10.7 ± 2.0	0.7 ± 0.1	<0.1	<0.1
60	117.7 ± 6.8	64.7 ± 1.6	15.1 ± 0.4	1.1 ± 0.4	0.2 ± 0.1	<0.1
			AHAP3			
10	24.6 ± 2.8	6.3 ± 0.3	0.5 ± 0.1	0.2 ± 0.1	<0.1	<0.1
20	37.6 ± 2.7	11.4 ± 0.6	0.5 ± 0.2	0.2 ± 0.1	<0.1	<0.1
40	160.7 ± 3.3	62.1 ± 3.1	6.5 ± 1.0	0.6 ± 0.2	0.3 ± 0.1	<0.1
60	222.0 ± 26.3	175.5 ± 17.9	13.0 ± 2.9	0.9 ± 0.1	0.6 ± 0.1	0.5 ± 0.1

<sup>a</sup> For each measurement,  $n \geq 3$ . Measurements obtained at physiological temperature and pH. <sup>b</sup> Detection limit of the instrument.

pH 7.4). A CH Instruments 900 electrochemical analyzer (Austin, TX) was used to apply a potential of +0.75 V (vs Ag/AgCl) to the working electrode. Sensor calibrations were performed before and after surface NO measurements using standard NO solutions. A NO stock solution was prepared daily by bubbling deoxygenated PBS with NO for 20 min to achieve a final NO concentration of 1.9 mM.<sup>25</sup> Surface concentration measurements were obtained by positioning the sensing tip at a distance of 10  $\mu\text{m}$  above the NO-releasing xerogel array using a computer-controlled inchworm motor (CH Instruments; Austin, TX). Current was measured for 10 min to obtain the steady-state level, which was then converted to NO concentration using the calibration curve.

## Results and Discussion

Sol-gel chemistry affords tremendous flexibility for preparing materials with tunable NO-release properties. We have previously reported on the synthesis of a range of xerogels with NO-release characteristics that are variable based on the type and concentration of the aminosilane NO-donor precursor, and the reaction/processing conditions.<sup>17,26,27</sup> Ethyltrimethoxysilane (ETMOS) sol-gels doped with varying concentrations of AEMP3, AEAP3, and AHAP3 were employed in the present study. Xerogels formed with ETMOS were smooth, glasslike, optically transparent, and comparable to previously reported aminosilane-containing isobutyltrimethoxysilane (BTMOS). Notably, the ETMOS sols were significantly less viscous and therefore more suitable for micropatterning than comparable BTMOS sols.<sup>27</sup>

**Xerogel Characterization.** The rates of NO release from uniform xerogel films synthesized with 10–60% (v/v, balance ETMOS) AEMP3, AEAP3, and AHAP3 were measured in real time and used to calculate NO surface flux. Stable, optically transparent xerogels could not be formed at aminosilane concentrations greater than 60%, and therefore such compositions were not pursued. As shown in Table 1, increasing the aminosilane concentration from 10 to 60% led to an increase in both the surface flux and duration of

NO release at physiological temperature. These findings are consistent with previous reports in which variable NO release profiles were achieved by altering the relative concentration of aminosilane in MTMOS and BTMOS networks.<sup>17,18,26–28</sup> Nitric oxide release was also variable depending on the type of aminosilane incorporated into the xerogel. Films doped with AHAP3 were characterized by the highest NO surface flux and duration of NO release, followed by AEAP3 and AEMP3, respectively. Such NO release behavior was expected based upon previous reports in which NO release rates (due to diazeniumdiolate decomposition) varied depending on the chemical structure of the amine precursor, with decomposition half-lives ranging from minutes to several days.<sup>21,27,28</sup> Hrabie et al. systematically evaluated the effects of diamine structure on diazeniumdiolate NO donor decomposition rates and found that increasing the length of the alkyl chain separating the amines led to an elevated rate of NO release.<sup>21</sup> The amines in AHAP3 are separated by a 6-carbon spacer versus a 2-carbon spacer for AEAP3 and AEMP3, which likely contributes to the observed NO-release trends from the xerogels. Furthermore, increasing the size of the organic group bound to the secondary amine has been demonstrated to lower the rates of NO release.<sup>21</sup> This size effect likely accounts for the lower fluxes of NO measured from AEMP3-modified xerogels. Indeed, analogous NO release trends have been reported for aminosilane-modified BTMOS xerogels.<sup>27,28</sup> Of note, negligible NO release was measured from control xerogels formed without aminosilane and bare glass substrates, thus the reported NO surface flux values represent NO generated from diazeniumdiolate decomposition and contributions from adsorbed NO are assumed to be insignificant.

To determine the effect of aminosilane type and concentration on xerogel surface wettability, static water contact angle measurements were obtained before and after NO exposure. As shown in Table 2, variations in aminosilane type and concentration did not affect the contact angle of the control films. These results are consistent with reports on the surface wettability of other aminosilane-containing xerogels,<sup>18,27</sup> and suggest that surface wettability is not

(25) *Handbook of Chemistry and Physics*; CRC Press: Boca Raton, FL, 1990–1991.

(26) Nablo, B. J.; Chen, T.-Y.; Schoenfish, M. H. *J. Am. Chem. Soc.* **2001**, *123*, 9712–9713.

(27) Marxer, S. M.; Rothrock, A. R.; Nablo, B. J.; Robbins, M. E.; Schoenfish, M. H. *Chem. Mater.* **2003**, *15*, 4193–4199.

(28) Rothrock, A. R.; Polizzi, M. A.; Brinkley, M. F.; Schoenfish, M. H. **2005**, in preparation.

**Table 2. Static Water Contact Angles for AEMP3, AEAP3, and AHAP3 (Balance ETMOS) Xerogel Films<sup>a</sup>**

% (v/v)	contact angle (deg)	
	control	NO-releasing
AEMP3		
10	84.8 ± 2.9	83.8 ± 1.8
20	85.0 ± 3.0	85.5 ± 2.2
40	88.6 ± 1.6	89.2 ± 1.5
60	88.4 ± 2.6	88.7 ± 0.7
AEAP3		
10	84.3 ± 2.8	87.2 ± 2.8
20	85.3 ± 2.2	87.1 ± 2.6
40	85.6 ± 2.8	88.7 ± 1.5
60	85.1 ± 2.9	88.2 ± 2.0
AHAP3		
10	85.2 ± 1.5	86.2 ± 1.8
20	86.6 ± 2.4	89.4 ± 2.3
40	90.0 ± 3.3	86.7 ± 2.2
60	90.6 ± 4.2	90.1 ± 2.9

<sup>a</sup> For each measurement,  $n \geq 3$ .

significantly affected by the presence of hydrophilic amine groups in the xerogel. Furthermore, NO exposure, and subsequent diazeniumdiolate NO donor formation, did not significantly alter surface wettability. Observed differences in the NO release profiles as a function of aminosilane type and concentration are thus attributed to variations in NO-donor formation and decomposition rates rather than variations in surface wettability.

Sol-gel chemistry allows for covalent attachment of the NO-donor to the xerogel matrix, thereby preventing leaching of the diamine precursor. Swelling or cracking of the xerogel under physiological conditions could, however, induce network fragmentation and present toxicity concerns. To assess material stability, xerogel films were immersed in Tyrode's buffer (pH 7.35) at 37 °C for periods up to 14 d. Network fragmentation was evaluated by measuring the concentration of Si in the soak solutions using DCP-OES. As shown in Table 3, regardless of aminosilane concentration, ETMOS films modified with AEMP3 exhibited minimal Si fragmentation, with measured values of  $<0.04 \mu\text{mol}\cdot\text{cm}^{-2}$  for up to 1 week. After two weeks of immersion, the measured Si fragmented from 60% AEMP3 (balance ETMOS) increased to  $1.18 \pm 1.11 \mu\text{mol}\cdot\text{cm}^{-2}$ , while fragmentation of ETMOS xerogels prepared with lower AEMP3 content remained below the instrument detection limit ( $0.04 \mu\text{mol}\cdot\text{cm}^{-2}$ ) over this interval. Similar to AEMP3/ETMOS films, the fragmentation of  $\leq 20\%$  AEAP3/ETMOS and AHAP3/ETMOS xerogels was negligible for the duration of the study. Increasing the aminosilane content to 40% resulted in films that were stable through 1 week with measured Si levels of only  $0.05 \pm 0.02$  and  $0.16 \pm 0.07 \mu\text{mol}\cdot\text{cm}^{-2}$  for AEAP3 and AHAP3, respectively. Increased fragmentation was observed after 2 weeks immersion for both aminosilanes. Xerogels prepared with 60% AEAP3 and AHAP3 (balance ETMOS) represented the least stable films, with Si concentrations of  $0.34 \pm 0.32$  and  $0.09 \pm 0.07 \mu\text{mol}\cdot\text{cm}^{-2}$ , respectively, after only 24 h immersion. These results are consistent with previous studies on the stability of both aminosilane-doped MTMOS<sup>18</sup> and BTMOS<sup>27</sup> xerogels which demonstrated an increase in xerogel network disruption as both the concentration of aminosilane and immersion time were increased. For subsequent experiments,

40% aminosilane-modified ETMOS xerogels were employed due to the optimal combination of stability and NO-release capability achieved with these materials.

**Ultraviolet Polymer Grafting.** The formation of xerogel micropatterns relies on capillary action of sol solution through an array of rectangular channels in an elastomeric PDMS template.<sup>17,18,29</sup> Thus, the rate of solution flow must be sufficiently rapid to ensure complete filling of the channels prior to gel formation.<sup>17,29,30</sup> The solution flow rate is governed by several factors including sol viscosity and the surface wettability of the channel walls.<sup>29-31</sup> The viscosity of MTMOS-based sols used in previous studies is relatively low compared with sols formed from other alkylsilanes (e.g., BTMOS and ETMOS), thus allowing for the formation of NO-releasing AEMP3/MTMOS xerogel micropatterns.<sup>17,18</sup> The NO-release capability of AEMP3/MTMOS xerogels is, however, significantly lower than that of comparable xerogels synthesized with AEAP3 and AHAP3; thus the utility of AEMP3/MTMOS arrays remains limited. Unfortunately, AEAP3/MTMOS and AHAP3/MTMOS xerogels, which would allow for enhanced NO release, cracked immediately upon immersion in solution.

Attempts to micropattern aminosilane-doped ETMOS sols using native PDMS were unsuccessful, presumably due to the hydrophobic nature of the channel walls. Previous work has shown that slightly increasing the template wettability via modification of the PDMS surface with the block copolymer PDMS-poly(ethylene glycol) (PDMS-PEG) facilitated successful patterning with MTMOS sols.<sup>17,18</sup> Unfortunately, the increased viscosity of ETMOS sols precluded the use of this method for micropattern preparation. To compensate for the viscosity of aminosilane-doped ETMOS sols and allow for the formation of NO-releasing ETMOS microarrays, the surface wettability of the PDMS template channels was systematically varied via ultraviolet polymer grafting. The structures of the hydrophilic graft monomers, acrylic acid (AA), dimethylacrylamide (DMA), and poly(ethylene glycol) acrylate (PEGA), employed for PDMS surface modification, are provided in Figures 2D-F. Monomers were selected on the basis of previous reports demonstrating the ability to vary hydrophilicity by covalently attaching these species via radicals formed on the surface of UV-exposed PDMS.<sup>20,32</sup> Surface grafting was achieved by immersing PDMS films and array templates in aqueous graft monomer solutions (10 wt %). Sodium periodate (0.5 mM) was added to the solutions to prevent oxygen from competing with monomers for reactive sites on the PDMS surface.<sup>33</sup> The addition of benzyl alcohol (1 wt %) served to enhance the efficiency of surface grafting by limiting homopolymerization of the monomers in solution.<sup>20,34</sup> Surface

(29) Kim, Y.; Park, C.; Clark, D. *Biotechnol. Bioeng.* **2001**, *73*, 331-337.

(30) Kim, E.; Xia, Y.; Whitesides, G. M. *J. Am. Chem. Soc.* **1996**, *118*, 5722-5731.

(31) Juncker, D.; Schmid, H.; Drechsler, U.; Wolf, H.; Wolf, M.; Michel, B.; de Rooij, N.; Delamarche, E. *Anal. Chem.* **2002**, *74*, 6139-6144.

(32) Hu, S.; Xueqin, R.; Bachman, M.; Sims, C. E.; Li, G. P.; Allbritton, N. L. *Langmuir* **2004**, *20*, 5569-5574.

(33) Uchida, E.; Uyama, Y.; Ikada, Y. *J. Appl. Polym. Sci.* **1989**, *41*, 677-687.

(34) Richey, T.; Iwata, H.; Oowaki, H.; Uchida, E.; Matsuda, S.; Ikada, Y. *Biomaterials* **2000**, *21*, 1057-1065.

Table 3. Direct Current Plasma Optical Emission Spectroscopy Analysis of ETMOS Xerogel Stability<sup>a</sup>

% (v/v)	fragmented Si ( $\mu\text{mol}\cdot\text{cm}^{-2}$ )				
	24 h	48 h	3 d	7 d	14 d
AEMP3					
10	<0.04 <sup>b</sup>	<0.04	<0.04	<0.04	<0.04
20	<0.04	<0.04	<0.04	<0.04	<0.04
40	<0.04	<0.04	<0.04	<0.04	<0.04
60	<0.04	<0.04	<0.04	<0.04	1.18 ± 1.11
AEAP3					
10	<0.04	<0.04	<0.04	<0.04	<0.04
20	<0.04	<0.04	<0.04	<0.04	0.07 ± 0.04
40	<0.04	<0.04	<0.04	0.05 ± 0.02	0.43 ± 0.09
60	0.34 ± 0.32	2.68 ± 2.04	5.14 ± 1.92	7.79 ± 1.60	11.97 ± 3.79
AHAP3					
10	<0.04	<0.04	<0.04	<0.04	<0.04
20	<0.04	<0.04	<0.04	<0.04	<0.04
40	<0.04	<0.04	0.04 ± 0.02	0.16 ± 0.07	0.53 ± 0.14
60	0.09 ± 0.07	0.20 ± 0.02	1.26 ± 0.54	1.72 ± 0.40	1.94 ± 0.32

<sup>a</sup> For each measurement,  $n \geq 3$ . Fragmentation measured at physiological temperature and pH. <sup>b</sup> Detection limit of the instrument.

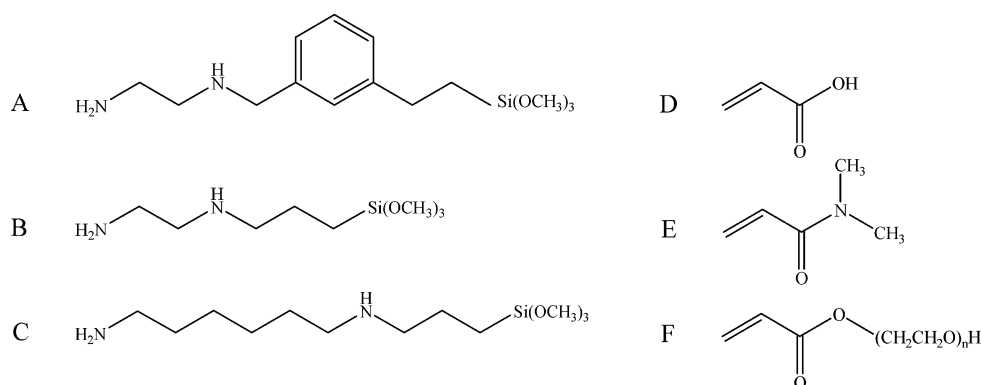


Figure 2. Structures of (A) AEMP3, (B) AEAP3, and (C) AHAP3 aminosilanes used to prepare NO-releasing xerogels, and (D) AA, (E) DMA, and (F) PEGA graft monomers used for template modification.

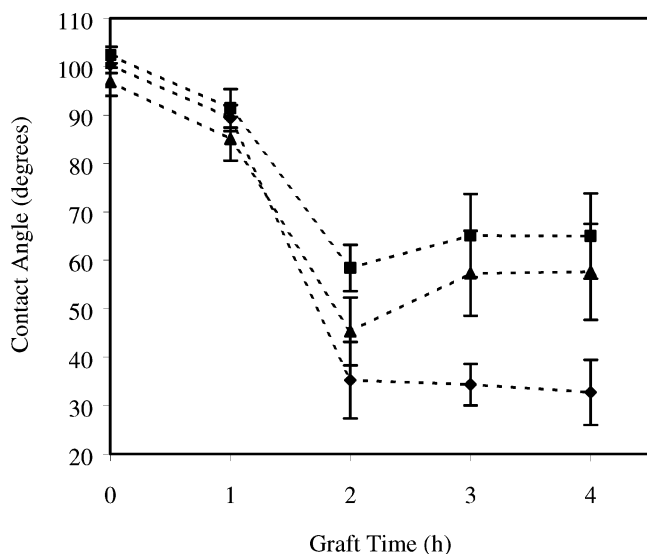


Figure 3. Effect of graft time on the surface wettability of PDMS modified with (◆) AA, (▲) PEGA, and (■) DMA graft monomers.

grafting was initiated by exposure of the immersed PDMS to UV light for periods ranging from 1 to 4 h. As shown in Figure 3, after 1 h of UV irradiation, a slight change in contact angle was observed for all graft monomers. After 2 h, significant changes in surface wettability were noted, with the most hydrophilic graft corresponding to AA followed by PEGA, and DMA. Longer graft times (beyond 2 h) did not lead to further reductions in contact angle; therefore, 2

h was determined to be the optimum graft polymerization time for subsequent studies. Surface grafting experiments were not conducted for periods longer than 4 h due to increased homopolymerization of the monomers in solution with time.

**Micropatterning Xerogels.** Although an assortment of xerogel microstructures can be prepared based on the geometry (e.g., rectangles, circles, squares, etc.) of the silicon master template, the arrays used in this study consisted of straight lines 4–8 mm long with widths and heights ranging from 10 to 50  $\mu\text{m}$  and 2 to 10  $\mu\text{m}$ , respectively. Individual microstructures were separated by 10–60  $\mu\text{m}$ . Xerogel arrays were prepared using previously described methods for patterning xerogel materials as shown schematically in Figure 1.<sup>17,18</sup>

Initial patterning attempts employed PDMS templates grafted with AA since the lowest water contact angles were achieved with this graft monomer. While ETMOS sols rapidly filled the array channels, detachment of the PDMS from the cured xerogel was not efficient, often resulting in damage to the micropattern. Such undesirable interactions (between the xerogel and grafted layer) can be attributed to the relatively high graft density of AA under these experimental conditions.<sup>20</sup> Attempts to form xerogel arrays with DMA-grafted PDMS were also unsuccessful, as the sol did not effectively enter the channels. The inability of the sol to fill the channels was attributed to the grafted PDMS being

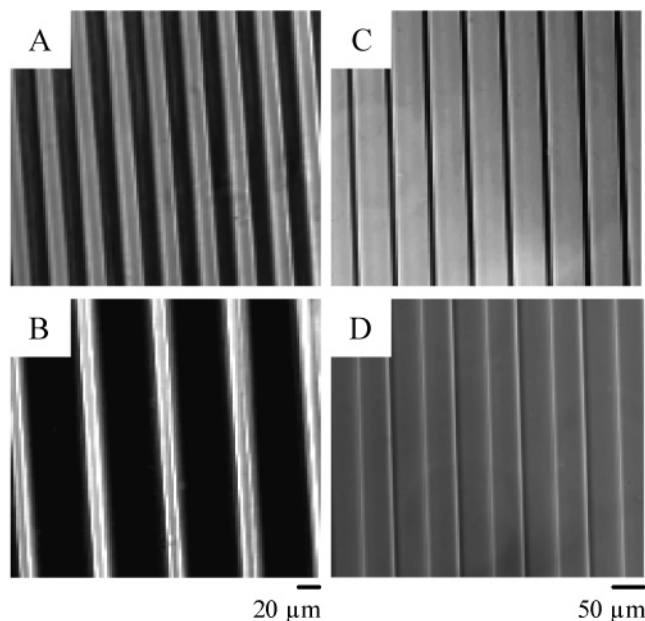


**Figure 4.** Representative phase contrast optical micrographs of 40% AHAP3 (balance ETMOS) xerogel lines (width = 20  $\mu\text{m}$ ; height = 10  $\mu\text{m}$ ) separated by distances of (A) 20  $\mu\text{m}$  and (B) 60  $\mu\text{m}$ , and 40% AEAP3 (balance ETMOS) xerogel lines (width = 50  $\mu\text{m}$ ; height = 10  $\mu\text{m}$ ) separated by distances of (C) 10  $\mu\text{m}$  and (D) 50  $\mu\text{m}$ . Arrays formed with PEGA-grafted PDMS templates.

insufficiently hydrophilic to overcome the flow resistance due to the sol viscosity, presumably due to the low graft density of this monomer.<sup>20</sup> Graft polymerization ( $t = 2$  h) with PEGA resulted in smooth, clear pattern templates with intermediate ( $45.3 \pm 4.8^\circ$ ) water contact angles. Sols prepared with up to 40% aminosilane (AEMP3, AEAP3, and AHAP3, balance ETMOS) rapidly filled the PEGA-modified channels. Furthermore, PEGA-grafted templates were easily removed from the cured xerogel. Representative phase-contrast optical micrographs of AEAP3 and AHAP3 micropatterns, formed with PEGA-grafted PDMS templates, are shown in Figure 4. The cured xerogel arrays were also characterized with atomic force microscopy before and after NO exposure. As expected from previous reports,<sup>17,18</sup> microstructure dimensions and root-mean-square (rms) roughness ( $\leq 10$  Å) were not altered by exposure to NO or buffer solution.

The stability of the grafted template with respect to surface wettability was evaluated to determine the optimum storage conditions for the treated PDMS prior to xerogel micropatterning. Studies by Hu et al. and Taniguchi et al. involving attenuated total internal reflectance infrared absorption (ATR-IR) spectra, surface wettability, graft density, and electroosmotic flow mobility measurements suggest that surface-grafted monomers are covalently bound to the template via reaction with radicals initiated on the PDMS surface by UV exposure.<sup>20,32,35</sup> However, reorientation of hydroxyl and methyl groups toward the bulk and surface of the PDMS, respectively, could result in variations in surface hydrophilicity with time.<sup>20,36</sup> Diffusion of low-molecular-

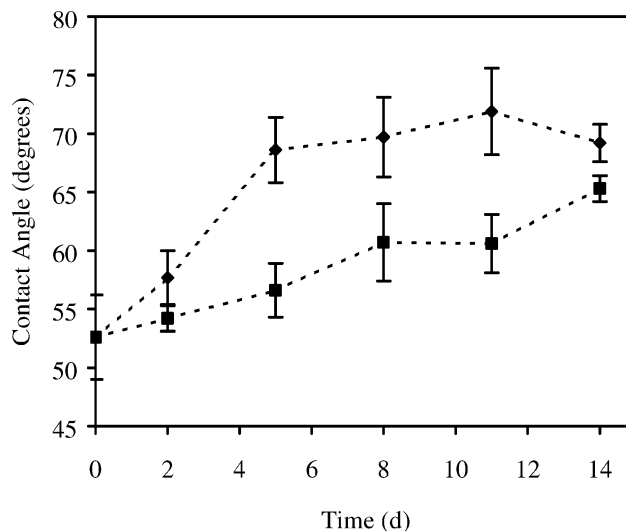


**Figure 5.** Effect of storage conditions on surface wettability of PEGA-grafted PDMS (2 h UV exposure). Samples were stored in (◆) air or (■) water at room temperature.

weight PDMS from the bulk to the surface may also lead to reduced wettability.<sup>20,36</sup> As shown in Figure 5, PEGA-grafted templates stored in water exhibited enhanced wettability (i.e., lower water contact angles) relative to samples stored in air. Within 5 d of air storage, the grafted surface was characterized by significantly higher water contact angles than samples immediately after grafting. Such behavior is not unexpected due to the reported dynamic nature of various polymer surfaces including PDMS.<sup>20,36,37</sup> Indeed, Holly and Refojo reported that poly(hydroxyethyl methacrylate) films expose methyl groups at the surface–air interface, whereas upon immersion in aqueous solution, the polymer reorients to expose hydrophilic hydroxyl groups.<sup>37</sup> Notably, attempts to form xerogel micropatterns with templates stored in air for  $\geq 5$  d were unsuccessful, presumably due to increased hydrophobicity from regions of exposed PDMS. Xerogel micropatterns were successfully formed using templates stored in water for up to 14 d. Although surface hydrophobicity did increase slightly with time for both air and water storage, even after 60 d (the longest period studied), the water contact angle values for both storage conditions was  $\sim 70^\circ$  and significantly lower than that of native PDMS ( $100^\circ$ ). Thus, the grafted PEGA is presumed to be intact over this interval and changes in surface wettability with time are attributed to variations in the exposed (ungrafted) portions of the PDMS surface.

**Nitric Oxide-Releasing Xerogel Micropatterns.** The surface flux and longevity of NO release from xerogels materials are easily tuned by varying the type (structure) and concentration of aminosilane precursors, and synthesis conditions.<sup>26,27</sup> Nitric oxide release properties are also adjustable based upon the microarray surface area dimensions.<sup>18</sup> Glass substrates were modified with a range of micropatterns prepared with 40% aminosilane (balance ETMOS). The arrays consisted of straight lines that were 10, 20, or 50  $\mu\text{m}$  wide, alternately spaced by distances ranging from 10 to 60  $\mu\text{m}$ . The xerogel lines were 10  $\mu\text{m}$  high and the total array

(35) Taniguchi, M.; Pieracci, J.; Samsonoff, W. A.; Belfort, G. *Chem. Mater.* **2003**, *15*, 3805–3812.

(36) Morra, A.; Occhiello, E.; Marola, R.; Garbassi, F.; Humphrey, P.; Johnson, D. *J. Colloid Interface Sci.* **1990**, *137*, 11–24.

(37) Holly, F. J.; Refojo, M. F. *J. Biomed. Mater. Res.* **1975**, *9*, 315–326.

**Table 4. Nitric Oxide Surface Flux ( $\text{pmol}\cdot\text{cm}^{-2}\cdot\text{s}^{-1}$ ) from Substrates ( $1\text{ cm}^2$ ) Modified with AEMP3, AEAP3, and AHAP3 (Balance ETMOS) Xerogel Arrays<sup>a</sup>**

SA ratio <sup>b</sup>	0 h	8 h	1 d	2 d	3 d	4 d
AEMP3						
0.7 <sup>c</sup>	3.9 ± 0.5	0.9 ± 0.3	0.8 ± 0.3	<0.1 <sup>f</sup>	<0.1	<0.1
0.9 <sup>d</sup>	6.3 ± 0.7	1.7 ± 1.0	1.0 ± 0.5	<0.1	<0.1	<0.1
1.0 <sup>e</sup>	10.2 ± 1.3	1.8 ± 0.3	1.0 ± 0.4	<0.1	<0.1	<0.1
AEAP3						
0.7	27.1 ± 2.7	2.3 ± 0.9	0.4 ± 0.2	0.2 ± 0.1	<0.1	<0.1
0.9	33.3 ± 3.4	13.2 ± 1.0	10.7 ± 0.4	3.2 ± 0.9	1.1 ± 0.2	<0.1
1.0	45.4 ± 1.2	13.5 ± 1.4	9.2 ± 3.0	2.9 ± 1.8	0.6 ± 0.3	0.2 ± 0.1
AHAP3						
0.7	53.0 ± 5.5	6.5 ± 1.1	0.6 ± 0.2	0.3 ± 0.1	<0.1	<0.1
0.9	64.0 ± 6.8	21.3 ± 2.9	21.2 ± 4.6	10.6 ± 3.8	0.7 ± 0.5	0.3 ± 0.1
1.0	73.6 ± 5.7	30.2 ± 7.3	29.0 ± 2.6	19.3 ± 7.6	3.7 ± 1.5	1.1 ± 1.0

<sup>a</sup> For each measurement,  $n \geq 3$ . Flux measured at physiological temperature and pH. <sup>b</sup> Surface area (SA) ratio of xerogel to exposed substrate. NOTE: SA = 1.0 indicates equal xerogel and substrate areas. <sup>c</sup> Array of xerogel lines with height = 10  $\mu\text{m}$ , width = 20  $\mu\text{m}$ , and separations alternating between 20, 40, and 60  $\mu\text{m}$ . <sup>d</sup> Array of xerogel lines with height = 10  $\mu\text{m}$ , width = 50  $\mu\text{m}$ , and separations alternating between 10, 25, and 50  $\mu\text{m}$ . <sup>e</sup> Array of xerogel lines with height = 10  $\mu\text{m}$ , width = 10  $\mu\text{m}$ , and separations alternating between 10, 25, and 50  $\mu\text{m}$ . <sup>f</sup> Detection limit of the instrument.

length was 8 mm. The surface flux and duration of NO release from these micropatterned substrates at physiological temperature and pH are reported in Table 4. Surface flux values ( $\text{pmol}\cdot\text{cm}^{-2}\cdot\text{s}^{-1}$ ) were calculated based on the total substrate surface area ( $1\text{ cm}^2$ ). For all aminosilanes, increasing the ratio of xerogel to unmodified glass resulted in an increased NO flux. Similar to xerogel films (Table 1), the surface flux and duration of NO release from AEMP3 microarrays were significantly lower than those of comparable AEAP3 and AHAP3 patterns. Indeed, 4- and 7-fold increases in initial NO surface flux values were achieved with AEAP3 and AHAP3 microarrays (SA ratio = 1), respectively. Previous in vitro experiments demonstrated that AEMP3 microarrays were effectively resistant to both platelet and bacterial adhesion at NO surface fluxes  $\geq 0.4\text{ pmol}\cdot\text{cm}^{-2}\cdot\text{s}^{-1}$ .<sup>15,17-19</sup> While these results are promising, in vitro experiments do not account for the numerous NO scavengers present in the body (e.g., proteins, thiols, transition metals, etc.) that would be expected to decrease the local concentration of NO.<sup>38</sup> Under these conditions, a higher NO surface flux may be required to impart biocompatibility. Thus, the increased surface flux values achieved with AEAP3 and AHAP3 xerogel micropatterns may be important in the application of these materials for in vivo devices. Furthermore, the duration of measurable NO release from AEAP3 and AHAP3 is double that of comparable AEMP3 xerogels. Previous in vitro studies have confirmed that the resistance of NO-releasing xerogels to both platelet and bacterial adhesion is diminished as the NO reservoir within the matrix becomes depleted with time.<sup>15,18,27</sup> Therefore, NO-releasing AEAP3 and AHAP3 xerogel arrays are likely to resist biofouling for longer periods than analogous AEMP3 micropatterns.

The reported surface flux values reflect the overall NO release characteristics of the micropatterned surfaces. To further investigate the NO release properties of AEAP3 and AHAP3 microarrays, localized surface concentration measurements were obtained using a NO-selective microelectrode sensor. In oxygenated media, NO is rapidly converted to nitrite, therefore obtaining accurate NO concentration mea-

**Table 5. Localized NO Surface Concentration (nM) for 40% AEAP3 and AHAP3 (Balance ETMOS) Arrays Measured with an Electrochemical NO Microsensor<sup>a</sup>**

array ( $\mu\text{m}$ ) <sup>b</sup>	1 h	24 h
AEAP3		
10:10	502 ± 24	57 ± 11
10:25	319 ± 29	42 ± 6
10:50	157 ± 31	15 ± 11
50:10	697 ± 12	87 ± 23
50:25	481 ± 21	37 ± 6
50:50	258 ± 32	16 ± 10
AHAP3		
10:10	527 ± 52	63 ± 13
10:25	450 ± 21	33 ± 7
10:50	331 ± 24	19 ± 2
50:10	751 ± 57	98 ± 12
50:25	587 ± 21	52 ± 10
50:50	345 ± 27	23 ± 13

<sup>a</sup> For each measurement,  $n \geq 3$ . Flux measured at physiological pH. <sup>b</sup> Microstructure dimensions reported as width/separation.

surements requires that the probe be positioned in close proximity to the xerogel surface to ensure a relatively short diffusion path length.<sup>39</sup> A probe-xerogel separation distance of 10  $\mu\text{m}$  was selected for NO concentration measurements.<sup>24</sup> The localized concentrations of NO produced from a variety of 40% AEAP3 and AHAP3 (balance ETMOS) xerogel microarrays are provided in Table 5. As expected, the highest NO concentration,  $751 \pm 57\text{ nM}$ , was generated from AHAP3 arrays consisting of 50- $\mu\text{m}$  wide lines separated by 10  $\mu\text{m}$ . At increased microstructure separations of 25 and 50  $\mu\text{m}$ , the NO surface concentrations decreased to  $587 \pm 21$  and  $345 \pm 27\text{ nM}$ , respectively. Lower levels of NO were measured above AHAP3 xerogel arrays consisting of 10- $\mu\text{m}$  lines separated by 10, 25, and 50  $\mu\text{m}$  distances. A decrease in NO concentration would be expected at reduced line widths for a constant line separation, since the fraction of unmodified glass (incapable of NO release) directly beneath the sensing tip increases. Analogous trends were observed for arrays formed with AEAP3. At increased immersion times, lower concentrations of NO were measured due to depletion of the finite NO donor reservoir within the xerogel microstructures.



Ramamurthi and Lewis reported that with NO concentrations as low as 0.4 nM, uniform biomaterial coatings are effectively resistant to platelet adhesion *in vitro*.<sup>40</sup> Micropatterns prepared with aminosilane-doped ETMOS xerogels may represent a unique platform for evaluating the localized concentrations of NO necessary to prevent cell adhesion to heterogeneous surfaces due to the broad range of NO release properties that may be achieved with these arrays. Experiments are currently underway to determine the optimum NO surface concentration, xerogel composition, and array dimensions/geometries for preventing platelet and bacterial cell adhesion to xerogel micropatterned interfaces.

### Conclusions

Results presented herein demonstrate that ultraviolet polymer grafting with PEGA is a viable strategy for modifying PDMS template wettability to allow for the micropatterning of xerogels with significantly greater NO release capability than previously reported xerogel micropatterns. The NO release properties of these ETMOS-based xerogels are easily varied based on the type and concentration of NO donor, and the micropattern dimensions employed

for surface modification. Chemiluminescence measurements confirmed that increasing the microarray surface area led to a corresponding increase in overall NO generation from micropatterned substrates. The localized NO surface concentrations, determined using a NO-selective microsensor, also varied based upon microarray dimensions, thus offering an additional parameter by which to tune the NO release properties of xerogel-modified substrates. Notably, the duration of NO release from AEAP3 and AHAP3 microarrays was double ( $\geq 96$  h) that of comparable AEMP3 arrays. These findings suggest that micropatterning NO-releasing AHAP3- and AEAP3-modified ETMOS xerogels may provide a means for enhancing substrate biocompatibility for significantly longer periods than previously described AEMP3/MTMOS arrays.

**Acknowledgment.** This research was supported by the National Institutes of Health (NIH EB000708). We gratefully acknowledge a Graduate Research Fellowship from the National Science Foundation (M.E.R.), a Linda Dykstra Science Dissertation Fellowship from The University of North Carolina at Chapel Hill Graduate School (M.E.R.), and a Smallwood Undergraduate Research Fellowship from the University of North Carolina at Chapel Hill Office of Undergraduate Research (E.D.H.).

CM050374X

---

(40) Ramamurthi, A.; Lewis, R. S. *Biomed. Sci. Instrum.* **1999**, 35, 333–338.